Health Signal Generation in the ORCA (Organic Robot Control Architecture) Framework

Raphael Maas and Erik Maehle

Institute of Computer Engineering
University of Lübeck
Ratzeburger Allee 160
D-23562 Lübeck, Germany
maehle@iti.uni-luebeck.de
maas@iti.uni-luebeck.de

Abstract: This paper evaluates various information-theoretical methods for the generation of health signals in the Organic Robot Control Architecture (ORCA). Also a new method based on the joint probability distribution of signals is proposed. The results show that the new method is superior to the known ones for the studied worst-case artificial and real scenarios. As an example for the application of health signals in ORCA, an adaptable path planner is described which considers the health status of a partially damaged robot.

1 Introduction

Autonomous mobile robots are becoming more and more complex in order to be able to execute more and more challenging tasks. Therefore, they also need sophisticated control systems which are able to master their complexity. With the complexity of a system the probability that it becomes faulty also increases. For mobile robots there are not only internal faults but also interaction faults with its environment. To ensure a high reliability and availability these faults have to be handled by the control system for achieving fault tolerance. Classical fault tolerance techniques which are mostly based on some kind of replication are, however, not suitable, since they require a considerable amount of additional redundant components which mean higher cost and energy consumption. Instead the natural redundancy of the system should be exploited and a fail-soft behaviour achieved.

Natural organisms show a high degree of fault tolerance in order to be able to survive. An example is the immune system which allows to checking the body for infections and reacts by destroying the intruders to restore health. Often self-organisation is used in organisms to allow a flexible response to abnormal situations. Organic computing is an approach to make these properties also available to complex embedded computing systems.

ORCA (Organic Robot Control Architecture) is a software framework developed at the University of Lübeck which supports the implementation of organic computing principles in particular for robotic systems. In ORCA so-called health signals are used to represent the health status of the robot. If the health signal drops, the control system reacts by organizing itself to continue the robot's mission in the best still possible way.

Thus, the generation of such health signals, which is the main subject of this paper, plays an important role in ORCA. Health signal generation is a very challenging task since it must be able to distinguish between normal healthy behaviour and abnormal faulty behaviour for very many, also unforeseen situations. An explicit fault model usually assumed in classical fault tolerance would become much too complex and is therefore not applicable.

Several concepts have already been proposed for health signal generation. One approach is inspired by the immune system and uses fuzzy rules with adaptable weights to detect abnormal situations [BrR08, JaM08]. Another concept is based on information theory and uses e. g. mutual information of signals for health signal generation [LJE07]. The latter approach will be further elaborated in this paper.

It has been an ongoing scientific interest to rate and measure the degree of information for given data sets in general. Different interpretations and approaches can be found in [HeQ95, PMV03, CoT06]. This includes for example varying normalizations of the mutual information like the ones presented in [LJE07] and [SHH99] that serve as a basis for this work.

The paper is organized as follows. First the ORCA framework is briefly presented in Chapter 2. Then the information-theoretical background used for health signal generation is given in Chapter 3. Besides already known approaches, also a new method based on the joint probability distribution of signals is introduced. To assess the quality of health signal generation, in Chapter 4 artificial worst case as well as real scenarios are evaluated for the proposed methods. Finally, Chapter 5 describes an example of the use of health signals for adaptable path planning for partially damaged robots.

2 Organic Robot Control Architecture (ORCA)

2.1 ORCA Framework

ORCA is a hierarchical and modular architecture which is based on two types of modules. Basic Control Units (BCUs) provide the basic functionality of the control system. The organic behaviour is implemented by separate Organic Control Units (OCUs). They constantly monitor the BCUs. In case OCUs detect an anomaly, they are able to change the behaviour of the BCUs so that the anomaly is handled in the best still possible way. The BCUs alone are sufficient to assure the functionality of the robot in the normal case, OCUs come only into play for abnormal situations.

Fig. 1 shows as simple example a differential drive of a wheeled mobile robot [MMG12]. There is a BCU on the drive layer which provides the interface of the drive to higher layers (not shown) with primitives like FORWARD, TURN LEFT, TURN

RIGHT etc. Its main function is to compute the corresponding speeds for the two motors which are given to separate motor controllers for the right and the left motor. These BCUs alone already implement the full functionality of the drive in the fault-free case. To support fault tolerance two additional OCUs are provided, one for each motor controller. They monitor their BCU for abnormal behaviour. If a motor shows e. g. a slower speed because it is damaged, they can counteract by changing the parameters like the set point of their motor controller.

ORCA has already been applied successfully to the walking robot OSCAR and allows it e.g. to continue walking even with damaged legs or to adapt to difficult terrain [MBG11].

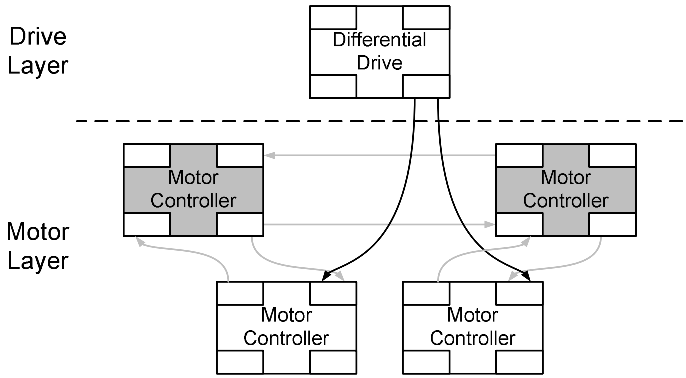

Figure 1: BCUs (white) and OCUs (gray) for a differential drive in ORCA. (Figure taken from [MMG12].)

2.2 Health Signals

An important concept of ORCA are health signals. They give an indication of the health status of a BCU which is monitored by an OCU. In abnormal situations the health signal drops and causes an OCU to intervene similarly to the natural immune system in case of an infection of the body. For the differential drive in Fig. 1 the motor controller BCUs generate a health signal which indicates the health state of their motors respectively. These health signals can be passed to other OCUs and combined to the health state on a higher layer, e. g. in the example in Fig. 1 for the whole drive.

3 Information-Theoretical Background

This chapter gives a brief introduction to the required information-theoretical background in section 3.1 by defining some basic identifiers and measures that are used to describe or rate signals. On this basis, section 3.2 presents special normalizations of the mutual information measure. Finally Section 3.3 introduces the signal classification

$\bar{C}_\omega$ as a measure to evaluate the similarity of two signals by analyzing their joint probability.

3.1 Signal Analysis

Let $S := (s_0, s_1, \dots, s_{t-1})$ be a discrete signal of length t, where s_z with $0 \leq z \leq t-1$ is the current value at time z. For each signal S there is a finite sample space $H_S := (Q_S, P_S)$. In this context $Q_S = \{(q_S)_0, (q_S)_1, \dots, (q_S)_{n-1}\}$ is the set of elementary events in S, where each item $(q_S)_i \in Q_S$ with $0 \leq i \leq n-1$ has a probability of occurrence $p((q_S)_i) \in [0,1]$ resulting in the vector $P_S := (p((q_S)_0), p((q_S)_1, \dots, p((q_S)_{n-1}))$. Hereafter p_i with $0 \leq i \leq n-1$ is used as a short form for $p((q_S)_i)$.

A visual representation of H_S is a histogram. This means that the elementary events in H_S are plotted against their respective probabilities.

Let $H_S = (Q_S, P_S)$ and $H_R = (Q_R, P_R)$ be the sample spaces of two signals S and R. The joint sample space of these signals is then given as $H_{SR} := (Q_S \times Q_R, P_{SR})$. The product set is defined as $Q_S \times Q_R := \left\{ \left((q_S)_i, (q_R)_j\right) \middle| \begin{matrix} i = 0, \dots, n-1 \\ j = 0, \dots, m-1 \end{matrix} \right\}$. Hereafter q_{ij} is used as a short form for $\left((q_S)_i, (q_R)_j\right)$ and p_{ij} stands for the joint probability $p\left(q_{ij}\right)$.

A visual representation of H_{SR} is a two dimensional histogram, where H_S is plotted against H_R and the joint probability of each possible combination is depicted as an intensity value.

The entropy of a given signal S is defined as $E_\alpha(H_S) := -\sum_{p_i \in P_S} p_i \log_\alpha p_i$, where α is used to set the base of the information measure. Common values of α are 2 (bit), e (nat) and 10 (Hartley) [HeQ95]. The joint entropy of two signals S and R is defined accordingly as $E_\alpha(H_{SR}) := -\sum_{p_{ij} \in P_{SR}} p_{ij} \log_\alpha p_{ij}$.

3.2 Mutual Information

Different definitions of the mutual information can be found throughout literature [HeQ95, PMV03, CoT06]. One possible definition focuses on the entropies of the involved signals and their joint entropy. In this context the mutual information is defined as $I_{\alpha(S,R)} := E_\alpha(H_S) + E_\alpha(H_R) - E_\alpha(H_{SR})$ and may reach maximal values if the joint entropy is minimal. It is furthermore possible to use normalized versions of the mutual information like $\hat{I}_\alpha(S,R) := \frac{I_\alpha(S,R)}{E_\alpha(H_S) \cdot E_\alpha(H_R)}$ [LJE07] or $\tilde{I}_\alpha(S,R) := \frac{E_\alpha(H_S) + E_\alpha(H_R)}{E_\alpha(H_{SR})}$ [SHH99].

In the context of health signal generation it is highly undesirable to use unbound measures like I_α and $\hat{I}_\alpha$. Therefore, this paper presents variants of these measures that are normalized with reference to a given signal. The goal of this approach is to achieve codomains that are bound by a [0, 1] interval. The basic idea of the normalization step is to scale a given mutual information measure with the best possible fit of two signals. This results in the following three definitions:

$$I_\alpha^S(S,R) \coloneqq \frac{I_\alpha(S,R)}{I_\alpha(S,S)}$$

$$\hat{I}_\alpha^S(S,R) \coloneqq \frac{\hat{I}_\alpha(S,R)}{\hat{I}_\alpha(S,S)}$$

$$\tilde{I}_\alpha^S(S,R) \coloneqq \frac{\tilde{I}_\alpha(S,R)}{\tilde{I}_\alpha(S,S)}$$

A detailed derivation can be found in [Maa14].

3.3 Signal Classification

As mentioned in section 3.1 the joint entropy of two signals can be represented as a two-dimensional histogram. The distribution of elementary events within such a histogram depends on the characteristics of the involved signals. If two signals have a perfect match, their elementary events occur only in identical pairs. Therefore the two-dimensional histogram of $H_{RR} \coloneqq (Q_R \times Q_R, P_{RR})$ exhibits a diagonal. The more two signals differ from each other, the more their elementary events migrate away from the diagonal. In the worst case all elementary events are equally spread across the whole histogram.

The basic idea behind the signal classification approach is to rate the deviation of each elementary event q_i from the diagonal $\vec{g}$ in the joint probability distribution. Fig. 2a gives a visual impression of this approach. The diagonal of a perfect match goes from the bottom left corner to the top right corner and is called $\vec{g}$. The spatial boundaries are given by the two points $(x_{\min}, y_{\min})$ and $(x_{\max}, y_{\max})$ which are the minimal and maximal elementary events of two signals X and Y. The deviation of q_i is measured as the perpendicular distance $|\vec{d_i}|$ of q_i to its foot on $\vec{g}$. This results in the fact that different maximal deviations are possible, depending on the position of the foot point. Fig. 2b illustrates this effect. As can be seen the vectors $\vec{l_i}$ and $\vec{l_j}$ show the relation $|\vec{l_i}| < |\vec{l_j}|$. For an actual rating in the context of health signals such a behaviour is undesirable because each elementary event should be considered with the same weight.

To smooth the weights of varying elementary events, the deviation of q_i is observed on a relative basis as $n_i \coloneqq \frac{|\vec{d}_i|}{|\vec{l}_i|}$. In this way the deviation is observed relative to its potential maximum. It has to be noted that this relation is only correct for square histograms, but is also used for rectangular histograms due to performance aspects.

Based on the previous considerations a precursor signal classification is defined as $C\,(S,R) \coloneqq \sum_{i=0}^{n-1} n_i p_i$ with $p_i \in P_{SR}$. Furthermore, a normalized version of this function is defined as $C_\omega(S,R) := \frac{C\,(S,R)}{\omega}$. This allows it to bind the classification to a range of [0, 1]. As a last step the final signal classification is defined as

$$\bar{C}_\omega(S,R) := 1 - C_\omega(S,R).$$

A detailed derivation of the signal classification and an appropriate allocation of ω can be found in [Maa14].

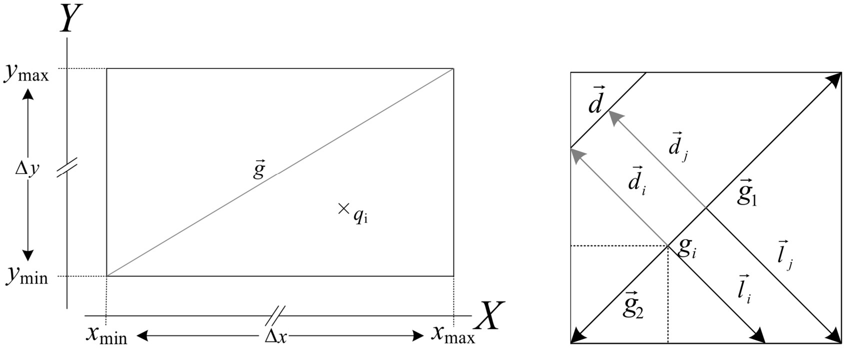

(a) Two-dimensional histogram (b) Distance relations

Figure 2: (a) shows a two-dimensional histogram for the two signals X and Y. The diagonal $\vec{g}$ represents a perfect match of X and Y. The elementary event q_i deviates from this match. (b) illustrates different maxima that occur for varying foot points on $\vec{g}$. (Figures taken from [Maa14].)

4 Health Signal Generation

This chapter presents test scenarios for the previously introduced methods for health signal generation. These methods are then evaluated and compared with a reference method for all test scenarios.

4.1 Methods

The basic idea of the information-theoretical approach is to use signal properties like entropy, mutual information or probability distribution to distinguish normal signals from abnormal ones and to compute a health signal based on the extent of the deviation.

A straight-forward approach to measure the similarity of two signals S and R is to simply compute the sum of absolute differences between them

$$\mathrm{SAD}(S,R) := \sum_{i=0}^{t-1} |s_i - r_i|,$$

which is in the following taken as a reference.

Furthermore, the three mutual information-based measures defined above

$$I_\alpha^S, \hat{I}_\alpha^S, \tilde{I}_\alpha^S$$

are used for health signals.

Also the new method for signal classification

$$\bar{C}_\omega(S, X)$$

which is based on the joint probability distribution of two signals S and X is evaluated.

4.2 Test Scenarios

In the following the quality of health signal generation for the information-theoretical approach shall be evaluated. For this purpose, nine representative scenarios are defined and the health signal generation according to the five methods described above are compared.

All scenarios assume three different observed signals:

- an optimal signal for the given situation
- a similar fault-free signal
- a faulty signal.

Scenarios 1 to 6 are artificial worst-case scenarios, scenarios 7 to 9 use real measurement data from damaged robots. In the first three scenarios and the real scenario 7 the abnormal signals differ in their levels form the normal ones, in scenarios 4 to 6 and 8 there is a loss of structure in the abnormal signal, e. g. due to noise. All scenarios are described in detail in [Maa14]. As an example scenario 9 is elaborated in the following.

A real mobile robot has been used for health signal generation (Fig. 3). It uses two kinds of sensors for obstacle avoidance: two ultrasonic distance sensors (US) on the left and right front side with the cones shown in Fig. 3 and an infrared distance sensor (IR) pointing in the forward direction with a very narrow cone pictured as a red line. The BCUs of the robot execute a simple reactive obstacle avoidance behaviour which is based on potential fields and vector addition. The resulting robot trajectory is represented by the dotted line. An OCU monitors the signals from the US and IR sensors. For the experiment, the average of the US sensor signals is taken as a fault-free reference signal S. The fault-free signal of the IR sensor is signal R_1 demonstrating a fault-free normal case. In order to inject a fault, the IR sensor is detached from its A/D converter resulting in a low level noisy signal R_2 for this abnormal case. All three signals are smoothed by a median filter to reduce noise and smooth signal inconsistencies that are caused by the layout of the sensors.

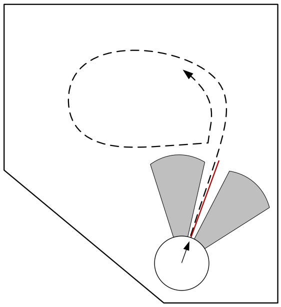

Figure 3: Mobile Robot with US- and IR-Sensors from Scenario 9. (Figure taken from [Maa14].)

4.3 Results

For the real world scenario 9 described above, the measured signal S for the optimal case, signal R_1 for the similar normal fault-three case and signal R_2 for the abnormal faulty case are shown in Fig. 4a. All three signals have a similar course until the fault is injected at $t = 858$. Then signal R_2 of the IR sensor drops to a low nearly constant level while the normal fault-free signals S and R_1 continue to run very similarly to each other while the robot continues moving.

In Fig. 4b to Fig. 4f the corresponding health signals according to the five methods presented in Chapter 4.1 are pictured. As can be seen all health signals react to the fault in R_2 by dropping, however, with different characteristics. For the fault-free sensor signal R_1, all health signals have a lower value than expected.

The two mutual information-based measures in Fig. 4b and 4d look similar and are able to clearly distinguish between the normal and abnormal situation. However, also in the fault-free case they only have a low health value although the system is healthy. This is better for Fig. 4c, but here the difference between the faulty and fault-free situations is not so clear any more. The SAD method in Fig. 4e has a rather high health signal as long as no fault occurs and then drops clearly. However, it later rises to a high level again though the fault is still there. As can be seen from Fig. 4a, this happens because the signal level for the fault-free sensors S is also very low from $t = 1150$ to 1500 resulting in only a small absolute difference to the faulty signal R_2. In summary, the health signal generation is not satisfactory for all these four methods.

The best results are observed for the new proposed probability distribution-based method in Fig 4f. It generates high health signal values for the normal case and clearly lower ones in case of the anomaly. It can be observed that $\bar{C}_\omega(S, R_2)$ shows a light reaction to the fault at first and then a strong reaction. This effect occurs because the signals were not completely assessed at once, but with a sliding window. The weaker reaction shortly after the fault can be explained by the fact that the window still holds fault-free values that keep the rating at a certain level. The health signal drops significantly, when the sliding window has gathered enough faulty data and the structure of the corresponding two-dimensional histogram changes.

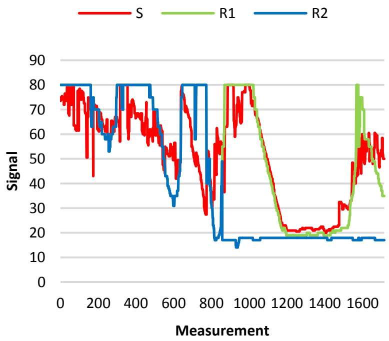

(a) Signals S, R_1 und R_2

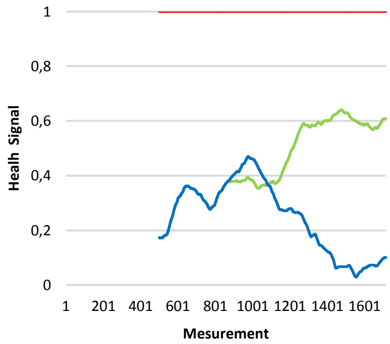

(b) $I_{10}^{S}(S, X)$

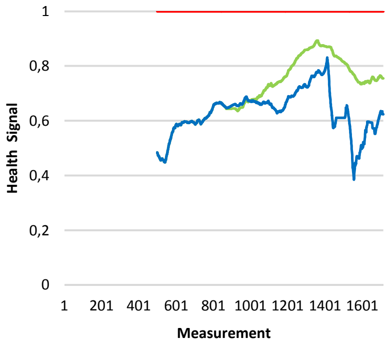

(c) $\hat{I}_{10}^{S}(S, X)$

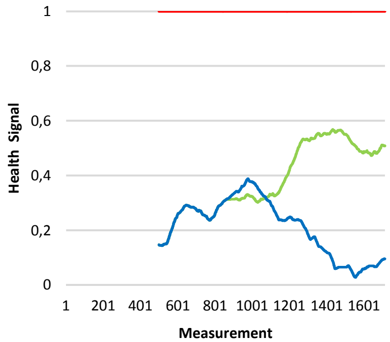

(d) $\tilde{I}_{10}^{S}(S, X)$

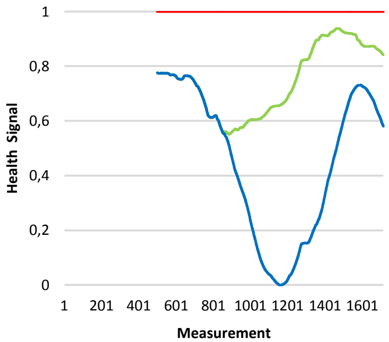

(e) $\mathrm{SAD}_{\omega}(S, X)$

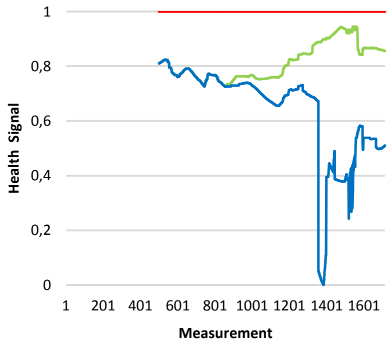

(f) $\bar{\mathrm{C}}_{\omega}(S, X)$

Figure 4: Results for Health Signal Generation in Scenario 9. (Figure based on [Maa14].)

A summary of all studied measures and all scenarios is shown in Tab. 1. Six categories are used to indicate the performance of all methods. If the resulting signals show positive and negative aspects the corresponding method is rated with $\pm$. Light tendencies to either positive or negative results are represented by $\oplus$ or $\ominus$. Strong tendencies are shown as $\oplus\oplus$ or $\ominus\ominus$. If a method is not applicable in a given scenario, it is marked with $\otimes$.

It can be seen that the new method based on joint probability distributions is superior to the three methods based on mutual information and SAD (Sum of Absolute Differences) for the studied scenarios. The measures based on mutual information are even worse than SAD in most cases and turn out to be not suitable for health signal generation.

Table 1: Summary of the Evaluation of Health Signal Generation for Scenario 1 to 9. (Figure based on [Maa14].)

Scenario	I_α^S	$\hat{I}_\alpha^S$	$\tilde{I}_\alpha^S$	SAD_ω	$\bar{C}_\omega$
1	$\otimes$	$\otimes$	$\otimes$	$\oplus$	$\oplus\oplus$
2	$\ominus\ominus$	$\otimes$	$\ominus\ominus$	$\oplus$	$\oplus\oplus$
3	$\otimes$	$\otimes$	$\otimes$	$\oplus$	$\oplus$
4	$\otimes$	$\otimes$	$\otimes$	$\otimes$	$\oplus$
5	$\ominus\ominus$	$\otimes$	$\ominus\ominus$	$\otimes$	$\oplus$
6	$\pm$	$\pm$	$\pm$	$\pm$	$\oplus$
7	$\otimes$	$\ominus\ominus$	$\ominus\ominus$	$\oplus$	$\oplus$
8	$\otimes$	$\ominus\ominus$	$\ominus\ominus$	$\oplus$	$\oplus$
9	$\pm$	$\pm$	$\pm$	$\pm$	$\oplus$

5 Adaptive Path Planning

In this chapter an outlook is given on how health signals can be used for adaptive path planning in difficult terrain for injured mobile robots (e.g. wheeled robots with damaged drives or walking robots with damaged legs [MBG11]). For this purpose, a classical wavefront-based path planner [BLL92, Jar95] is executed by a BCU. In case of a lowered health signal, the OCU modifies the map of the terrain by changing those areas which are too difficult to pass for the current health status of the robot into obstacles. Thus the BCU replans the path around them (see Fig. 5). A detailed description and evaluation of different approaches can be found in [MaM11, Maa14].

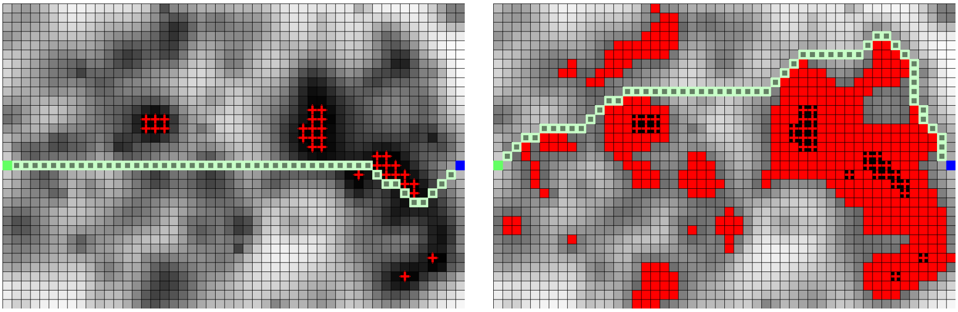

Figure 5: Adaptive Path Planning for a mobile robot based on health signals (left: 100% healthy, right 90% healthy). Difficulties of the terrain are shown as grey levels, obstacles in red. (Figure taken from [Maa14].)

6 Conclusion

This paper has presented an evaluation of the quality of health signal generation for various information-theoretical methods in the ORCA framework. Health signals are used in ORCA by Organic Control Units (OCUs) in order to describe the health status of Basic Control Units (BCUs) monitored by them. It turned out that SAD as well as known mutual information-based measures do not always yield satisfactory results. Only a newly proposed method based on the joint probability distribution of signals showed the desired properties. It was also presented how health signals can be used to plan a suitable path through difficult terrain so that even partly damaged robots can reach their goal.

Future comparative studies should also include other than information-theoretical methods like e.g. fuzzy rule sets. Moreover, it needs to be studied further which information about the health status of a BCU is actually required by higher levels like the path planner. The health signal alone only gives a quantitative measure on how healthy a robot is but does not say what kind of damage it has and what capabilities still remain. Therefore, it can be desirable that the OCUs at higher levels are able to request this information from OCUs at lower levels.

Acknowledgement

This work was funded in part by the German Research Foundation (DFG) within the priority programme Organic Computing (1183) under grant reference MA 1412/8-2.

References

[BrR08] Brockmann, W.; Rosemann, N.: Instantaneous anomaly detection in online learning fuzzy systems. In: Workshop on Genetic and Evolving Systems (GEFS). 2008; p. 23-28.

[JaM08] Jakimovski, B.; Maehle, E.: Artificial Immune System Based Robot Anomaly Detection Engine for Fault Tolerant Robots. In: Autonomic and Trusted Computing, Lecture Notes in Computer Science, 5060, 2008. Springer Berlin, Heidelberg. 2008; p. 177-190.

[LJE07] Larionova, S.; Jakimovski, B.; El Sayed Auf, A.; Litza, M.; Moesch, F.; Maehle, E.; Brockmann, W.: Toward a Fault Tolerant Mobile Robot: Mutual Information for Monitoring of the Robot Health Status. In: International Workshop on Technical Challenges for Dependable Robots in Human Environments. IEEE/RAS, 2007; p. 1-5.

[HeQ95] Heise, W.; Quattrocchi, P.: Informations- und Codierungstheorie, Springer Berlin Heidelberg, 1995.

[PMV03] Pluim, J. P. W.; Maintz, J. B. A.; Viergever, M. A.: Mutual-information-based registration of medical images: a survey. In: Transactions on Medical Imaging, Vol. 22, No. 8. IEEE, 2003; p. 986-1004.

[CoT06] Cover, T. M.; Thomas, J. A.: Elements of Information Theory, John Wiley & Sons, 2006.

[SHH99] Studholme, C.; Hill, D. L. G.; Hawkes, D. J.: An overlap invariant entropy measure of 3D medical image alignment. In: Pattern Recognition, Vol. 32, No. 1. 1999; p. 71-86.

[MMG12] Maas, R.; Maehle, E.; Großpietsch, K. E.: Applying the Organic Robot Control Architecture ORCA to Cyber-Physical Systems. In: EUROMICRO Conf. on Software Engineering and Advanced Applications (SEAA), 2012. IEEE, 2012; p. 250-257.

[MBG11] Maehle, E.; Brockmann, W.; Großpietsch, K.-E., El Sayed Auf, A.; Jakimovski, B.; Krannich, S.; Litza, M.; Maas, R.; Al-Homsy, A.: Application of the Organic Robot Control Architecture ORCA to the Six-legged Walking Robot OSCAR. In: Organic Computing - A Paradigm Shift for Complex Systems. Birkhäuser-Springer, Basel 2011; p. 517-530.

[Maa14] Maas, R.: Adaptive Kontrollstrategien für mobile Roboter basierend auf Organic Computing Prinzipien, University of Lübeck, 2014 (to appear).

[BLL92] Barraquand, J.; Langlois, B.; Latombe, J.: Numerical Potential Field Techniques for Robot Path Planning. In: Trans. on Man and Cybernetics, 22. IEEE, 1992; p. 224-241.

[Jar95] Jarvis, R.: Collision Free Trajectory Planning Using Distance Transforms. In: Mechanical Engineering Transactions, ME10. 1995; p. 187-191.

[MaM11] Maas, R.; Maehle, E.: Fault Tolerant and Adaptive Path Planning for Mobile Robots Based on Health Signals. In: International Conference on Architecture of Computer Systems (ARCS) 2011, Workshop Proceedings. VDE Verlag, 2011; p. 58-63.